JACS
JOURNAL OF THE AMERICAN CHEMICAL SOCIETY

Subscriber access provided by BUFFALO STATE

Article

Combining Synthesis and Self-Assembly in One Pot to Construct Complex 2D Metallo-Supramolecules Using Terpyridine and Pyrylium Salts

Heng Wang, Yiming Li, Hao Yu, Bo Song, Shuai Lu, Xin-Qi Hao, Yuan Zhang, Ming Wang, Saw-Wai Hla, and Xiaopeng Li

J. Am. Chem. Soc., **Just Accepted Manuscript** • Publication Date (Web): 25 Jul 2019

Downloaded from pubs.acs.org on July 25, 2019

Just Accepted

"Just Accepted" manuscripts have been peer-reviewed and accepted for publication. They are posted online prior to technical editing, formatting for publication and author proofing. The American Chemical Society provides "Just Accepted" as a service to the research community to expedite the dissemination of scientific material as soon as possible after acceptance. "Just Accepted" manuscripts appear in full in PDF format accompanied by an HTML abstract. "Just Accepted" manuscripts have been fully peer reviewed, but should not be considered the official version of record. They are citable by the Digital Object Identifier (DOI®). "Just Accepted" is an optional service offered to authors. Therefore, the "Just Accepted" Web site may not include all articles that will be published in the journal. After a manuscript is technically edited and formatted, it will be removed from the "Just Accepted" Web site and published as an ASAP article. Note that technical editing may introduce minor changes to the manuscript text and/or graphics which could affect content, and all legal disclaimers and ethical guidelines that apply to the journal pertain. ACS cannot be held responsible for errors or consequences arising from the use of information contained in these "Just Accepted" manuscripts.

is published by the American Chemical Society. 1155 Sixteenth Street N.W., Washington, DC 20036

Published by American Chemical Society. Copyright © American Chemical Society. However, no copyright claim is made to original U.S. Government works, or works produced by employees of any Commonwealth realm Crown government in the course of their duties.

Combining Synthesis and Self-Assembly in One Pot to Construct Complex 2D Metallo-Supramolecules Using Terpyridine and Pyrylium Salts

Heng Wang,[†] Yiming Li,[†] Hao Yu,[‡] Bo Song,[†] Shuai Lu,[†,§] Xin-Qi Hao,[§] Yuan Zhang,[∥] Ming Wang,[‡] Saw-Wai Hla,[∥] Xiaopeng Li*,[†]

[†]Department of Chemistry, University of South Florida, Tampa, Florida 33620, United States

[‡]State Key Laboratory of Supramolecular Structure and Materials, College of Chemistry, Jilin University, Changchun, Jilin 130012, China

[§]College of Chemistry and Molecular Engineering, Zhengzhou University, Zhengzhou, Henan 450001, China

[∥]Nanoscience and Technology Division, Argonne National Laboratory, Lemont, Illinois 60439, USA

KEYWORDS pyrylium salts, terpyridine, supramolecular chemistry, multi-component self-assembly

ABSTRACT: Multi-component self-assembly in one-pot provides an efficient way for constructing complex architectures using multiple-type of building blocks with different levels of interactions orthogonally. The preparation of multiple-type of building blocks typically include tedious synthesis. Here, we developed a multi-component synthesis/self-assembly strategy, which combined covalent interaction (C—N bond, formed through condensation of pyrylium salt with primary amine) and metal-ligand interaction (N→Zn bond, formed through 2,2′:6′,2″-terpyridine-Zn coordination) in one pot. The high compatibility of this pair of interactions smoothly and efficiently converted three and four types of components into desired complex structures, i.e., supramolecular Kandinsky circles and spiderwebs, respectively.

Introduction

Nature, as a talent programmer, codes extremely sophisticated life information into proteins and DNAs through combining multi-component *in-situ* reactions with multi-level of non-covalent (hydrogen bonding, π-π, dipole-dipole, etc.) and covalent (amidations or esterifications) interactions in one biological system.[1] Formation of discrete assemblies from a pool of building block through "order-out-of-chaos" approaches is emerging as one of the ultimate goals of synthetic supramolecular chemistry in pursuing higher level of complexity and desired functionalities.[2] Among the diverse research fields of supramolecular chemistry, coordination-driven self-assembly benefiting from its highly directional and predictable feature has been extensively applied to construct a vast variety of supramolecular architectures,[3] including helicates,[4] grids,[5] rotaxanes,[6] catenanes,[7-9] links,[10] knots,[11] polygons,[12-14] and polyhedra.[15-17] However, most of these studies focused on building up metallo-supramolecules via a single type of organic building block.

To achieve more sophisticated supramolecular systems with higher efficiency, great efforts have been made on multi-component self-assembly, such as social self-sorting to compose a series of heteroleptic coordination sites,[16e, 18-20] subcomponent self-assembly based on reversible imine bond formation and metal-ligand coordination,[17f, 17g, 21] template driven synthesis of discrete supramolecules,[22, 23] etc. These one-pot strategies rather than combining all building blocks in a presynthesized ligand dramatically reduced the barrier in ligand design and synthesis. However, rational design of different levels of interactions in an orthogonal manner to minimize unwanted products is still full of challenges in the multi-component system and thus, limits the complexity of metallo-supramolecules for further advancement of functionality.

Beyond those boundaries, we herein developed a multi-component synthesis/self-assembly strategy, which enabled the construction of double layered supramolecular Kandinsky Circles (**KC**) with three components, and supramolecular spiderwebs with four components in one-pot. Unlike subcomponent and template driven synthetic strategies, such an attempt combined an *irreversible* condensation of pyrylium salt and primary amine[24] together with highly reversible 2,2′:6′,2″-terpyridine (tpy)-Zn(II) coordination processes[25] in one-pot *without any assistance from templates*. This new approach not only improved the synthetic efficiency of desired supramolecules with increasing complexity, but also enriched the library of the multi-component self-assembly.

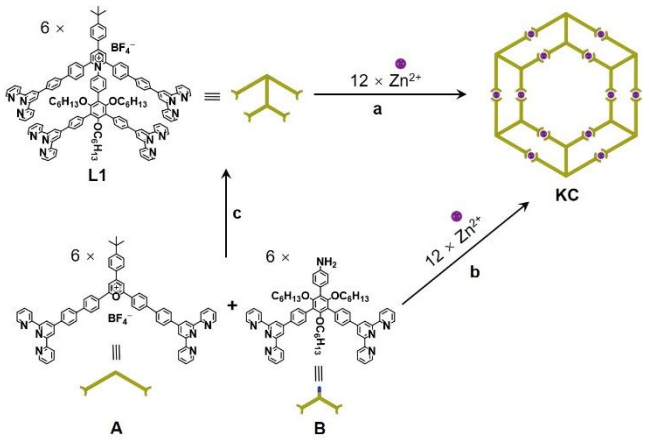

Scheme 1. Preparation of KC. (a) Conventional self-assembly using presynthesized ligand **L1**; condition: $CHCl_3$/MeOH (1/3, v/v), 50 °C, 3 hours. (b) One-pot approach with synthesis and self-assembly together using precursors **A** and **B**; condition: DMSO, 110 °C, 24 hours. (c) Synthesis of L1 from **A** and **B**, condition: DMSO, 120 °C, 24 hours.

Results and Discussion

Self-assembly of double layered KC via one-pot strategy. In our previous work, we assembled multi-layered **KC**s using multi-topic tpy-pyridinium salts through multi-step synthesis.[14j, 14k] Such **KC**s exhibited remarkable antimicrobial activity against Gram-positive pathogen methicillin-resistant *Staphylococcus aureus* (MRSA). However, the tedious synthesis and challenging purification of the charged multiarmed tpy-pyridinium ligands limited the investigations of their properties and applications. As a result, instead of using the conventional strategy (Scheme 1a), we tried to explore the possibility of directly constructing **KC** through two precursors, i.e., pyrylium salt **A** and primary amine **B**, with proper portion of Zn(II) in one-pot (Scheme 1b). We hypothesized that the condensation and the tpy-Zn coordination could be orthogonal to facilitate this new type of *in-situ* multicomponent synthesis/self-assembly. We speculated the following three circumstances might occur: i) no condensation happens, and a mixture of numerous mono-layered circles is assembled by **A**/**B** with Zn(II) narcissistically or socially; ii) condensation partially occurs, and a mixture of ligand **L1** and unreacted **A**/**B** form random polymeric metallo-assemblies; iii) **A** and **B** are fully converted, and the multi-component synthesis/assembly perfectly generates a desired discrete structure.

Precursors **A**/**B** and $Zn(NO_3)_2$ were mixed in DMSO with the stoichiometric ratio (1/1/2). After 24 hours heating at 110 °C, the assembly was precipitated by adding excess amount of NH_4PF_6 methanol solution, collected after simple methanol wash, and directly subjected for characterization without further purification. Electrospray ionization-mass spectrometry (ESI-MS) was first utilized to address the molecular composition of the obtained assembly. Mass spectrum (Figure 1a) showed one dominant set of peaks with continuous charge state from 11+ to 24+, suggesting a discrete supramolecular structure was obtained during the one-pot synthesis/self-assembly. After deconvolution of each peak, the measured molecular mass of the obtained supramolecule was 17,413 Da in average, which exactly matches the molecular composition of **KC** [$C_{846}H_{732}O_{18}N_{78}Zn_{12}P_{30}F_{180}$]. The experimental isotope pattern of each charge state also agrees well with their theoretical simulations based on the chemical composition of **KC** (Figure 1 insert, Figure S33). Traveling wave ion mobility-mass spectrometry (TWIM-MS)[14k, 26] spectrum presents a series of signals with narrow bands attributed to **KC** species with successive charge state, indicating high isomeric purity of the composed structure. NMR spectra including ^{1}H, COSY and NOESY were collected (Figures S5-11) and carefully compared with the results collected from the supramolecule assembled via presynthesized ligand strategy.[14j] No significant difference was observed between the supramolecules prepared through these two strategies (Figure S5), suggesting that the condensation and coordination were compatible and orthogonal in such a one-pot manner.

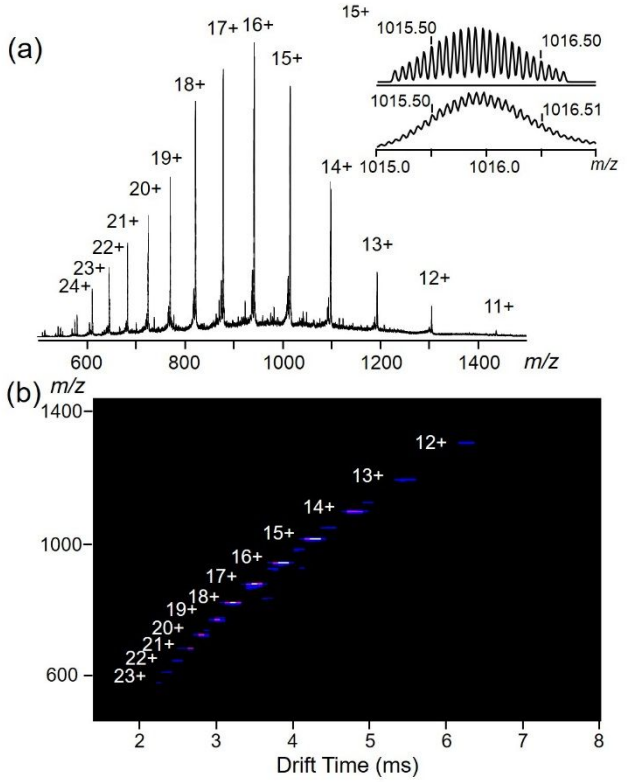

Figure 1. (a) Full ESI-MS spectrum with theoretical and experimental isotope patterns of 15+ species (right inset). (b) TWIM-MS (*m/z vs* drift time) of **KC** composed by three-component in-situ self-assembly strategy.

Carefully identifying the compositions among the reaction mixture at each reaction stage offered us more detailed information on understanding the mechanism of the *in-situ* synthesis and self-assembly. ESI-MS was utilized to monitor the assembly process, and results are shown in Figure 2. At the earliest reaction stage (15 min after the reaction mixture being heated at 110 °C, in order to dissolve all reactants), an extremely messy spectrum was observed with most peaks in the range of *m/z* 500~900, but no peak

was detected for **KC**. Detailed analysis of these peaks indicated that a mixture of **B**-Zn(II) macrocycles and **A**-**B**-Zn(II) macrocycles was formed at the very beginning of the self-assembly (Figures S41a, b, Scheme S3a). Intriguingly, **A-B** condensation intermediate, [**A-B**] (structure was shown in Scheme S3b), was found to be assembled with Zn(II) along with various amount of additional **A** and/or **B** (Figures S41c, d, Scheme S3b-c). Such multiple entities were regarded as the intermediate species prior to the formation of our desired **KC** structure. After two hours of heating, several peaks assigned to **KC** were observed and gradually enhanced with increasing reaction time. Compared to the rising of the sharp peaks of **KC**, all the other messy peaks shrank and completely disappeared after 24 hours of heating, indicating a complete conversion of **A**/**B** to form **KC** (Figure 2).

We gradually lowered the temperature from 110 °C to 50 °C to monitor the conversion process using ESI-MS, which showed a significant increase of full conversion time (Figures S42-44). The full conversion time for each reaction temperature is 24 h at 110 °C, 60 h at 90 °C, 164 h at 70 °C, and 456 h at 50 °C. Along with the conversion of the intermediate species, clean sets of peaks of **KC** were observed under all temperature conditions without other impurities observed.

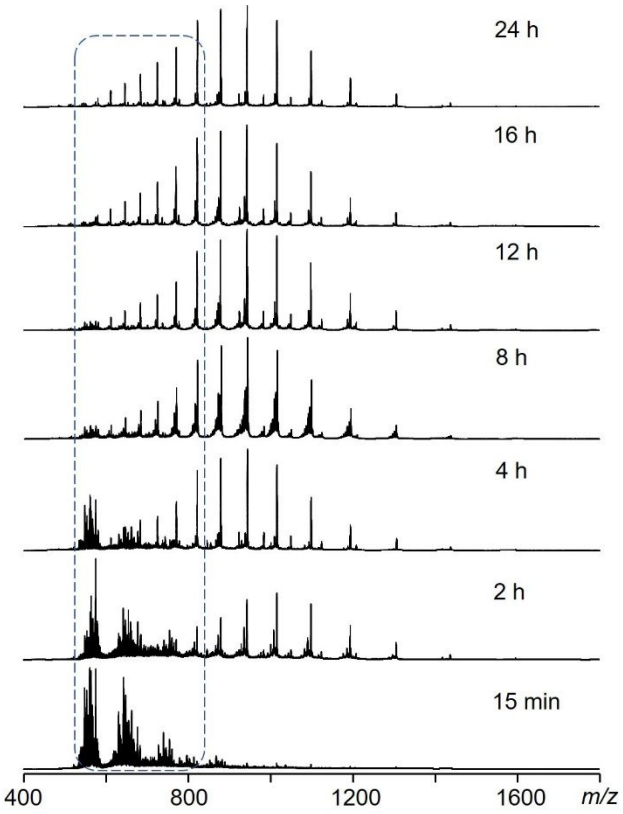

Figure 2. One-pot synthesis of **KC** at 110 °C monitored via ESI-MS at various reaction time.

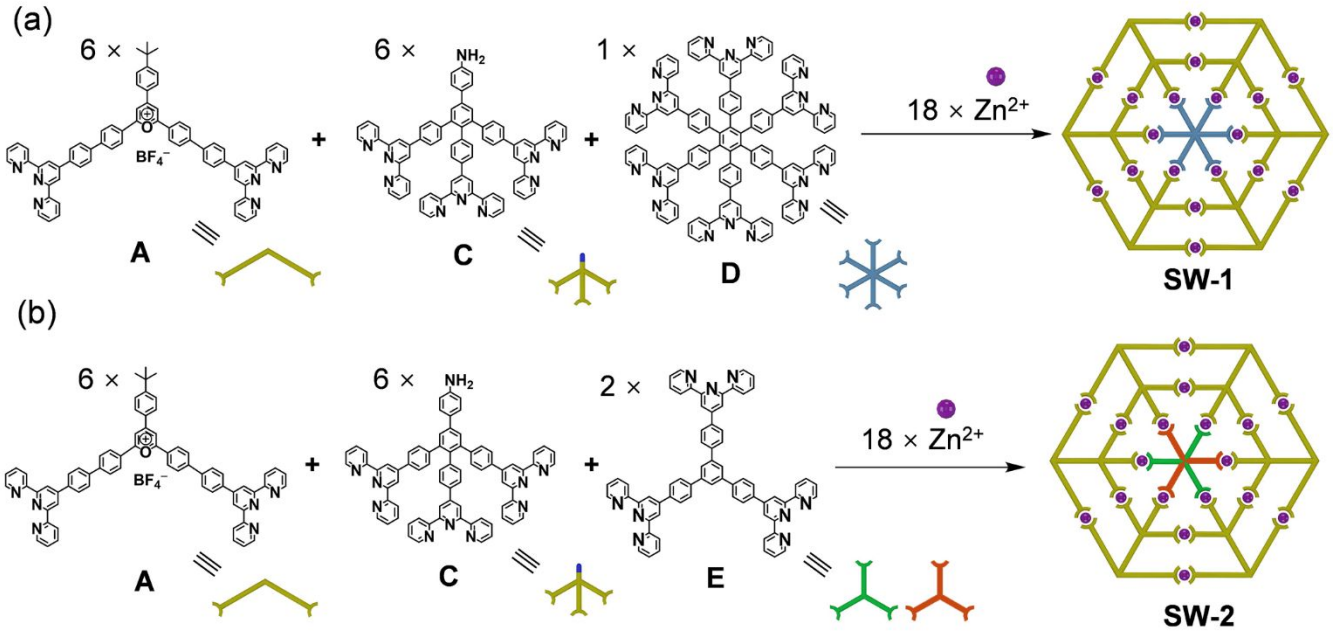

Scheme 2. Preparation of (a) SW-1 and (b) SW-2 through four-component synthesis/self-assembly in one pot. Condition: DMSO, 110 °C, 24 hours.

Self-assembly of Spiderweb-like supramolecules (SW-1 and SW-2) via one-pot strategy. To test the versatility of this new one-pot strategy, we could design even more complex supramolecules by simply changing organic precursors. For instance, a spiderweb-like (**SW-1**) supramolecule can be constructed by replacing precursor **B** with a tritopic tpy ligand **C** and adding hexatopic tpy ligand **D** acting as a core in a four-component synthesis/self-assembly (Scheme 2a). **SW-1** was constructed by using the same procedure of preparing **KC**. Only one dominant set of

sharp peaks is observed in the ESI-MS spectrum (Figure 3) with various charge states (11+ to 24+). And the isotope pattern of each charge state peak also agrees well with the corresponding theoretical simulation result (Figure 3 insert and Figure S34). The averaged molecular mass was deconvoluted as 21,508 Da, which matches the chemical composition ($C_{996}H_{678}N_{114}Zn_{18}P_{42}F_{252}$). Furthermore, TWIM-MS spectrum shows a series of narrowly distributed signals, which indicates no isomers or conformers were formed during the self-assembly. Collision cross sections (CCSs),[26b, 26c] which are determined by the shape and size of molecules, are derived through the drift time of **SW-1** species with various charge state (results are summarized in Table S2, Figure S48). The averaged measured CCSs is 2817.0 Å^2, which is in good agreement with the calculated CCSs result (2826.9 Å^2) of **SW-1**. Note that the CCS of **SW-1** is slightly larger than that of **KC** (2466 Å^2).[14j] The excess CCS value should come from the additional core structure of **SW-1** compared with **KC**. Further stability characterization in gas phase was carried out by gradient tandem mass spectrometry (gMS^2)[26] under various collision energies, as shown in Figure S39. The 15+ ions of **SW-1** totally dissociated at 40 V, corresponding to a center-of-mass collision energy at 0.08 eV. The dissociation voltage is much higher than the corresponding total dissociation voltage of 15+ ions of **KC** (30 V, center-of-mass collision energy at 0.07 eV, Figure. S36), indicating a higher stability of **SW-1** than **KC** (in gas phase). Such enhanced stability is attributed to the higher density of coordination sites (DOCS) of **SW-1** (0.0064 site/Å^2) than **KC** (0.0047 site/Å^2).[27]

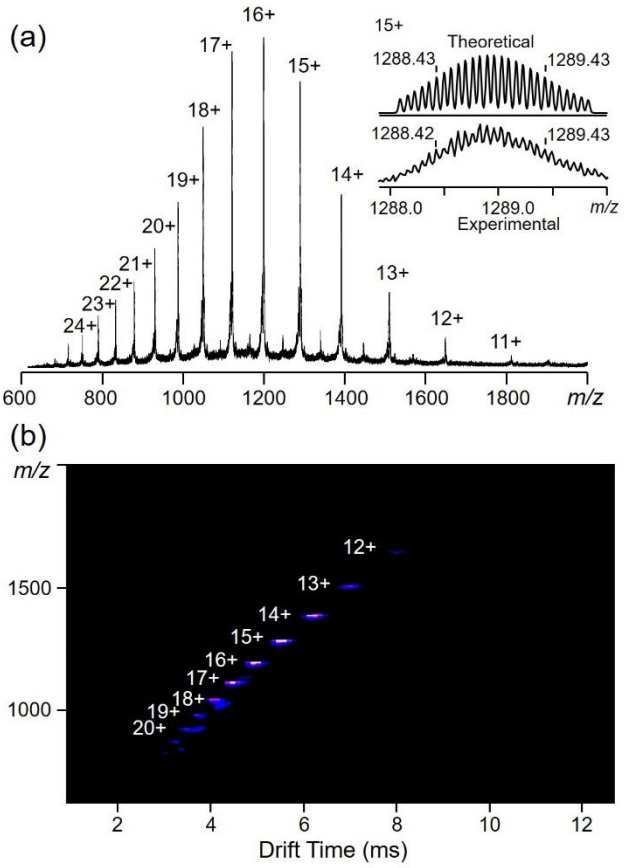

Figure 3. (a) Full ESI-MS spectrum with theoretical and experimental isotope patterns of 15+ species (right inset). (b) TWIM-MS (*m/z vs* drift time) of **SW-1** composed by four-component *in-situ* self-assembly strategy.

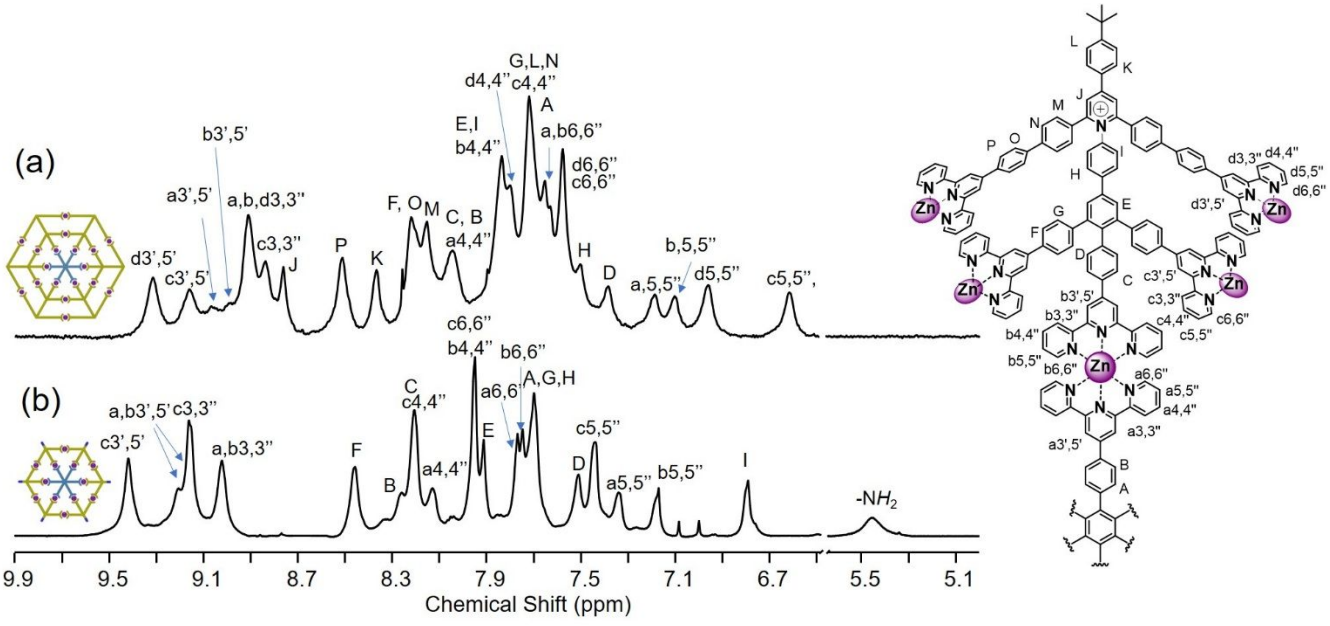

Figure 4. ^{1}H NMR spectra (600 MHz, d_6-DMSO, 300 K) of (a) **SW-1** and (b) **SW-3**.

Apart from the one-pot strategy, another step-wise approach was also employed to construct **SW-1**. The step-wise approach was illustrated in Scheme S2. Precursors **C** and **D** were assembled with stoichiometric amount of Zn(II) to produce a discrete supramolecular spokewheel (**SW-3**)[28] with 6 reactive amino groups around the rim. ESI-MS of **SW-3** (Figure S36) displays one dominant set of sharp peaks with continuous charges ranged from 8+ to 18+, as well as well resolved isotope patterns (Figure S37). The deconvoluted molar mass is 12,733 Da, matching its chemical composition. Then, precursor **A** and additional amount of Zn(II) were added into **SW-3** solution. ESI-MS showed that **SW-1** was smoothly formed with the exactly same ESI-MS spectrum as the one-pot method (Figure S45). Such results further support the high orthogonality of the tpy-Zn(II) coordination with the condensation reaction.

Figure 4 shows the ^{1}H NMR spectra of **SW-1** and **SW-3**, which provides more detailed structural information. In the spectra of **SW-3**, three sets of peaks assigned to the protons on the tpy groups can be figured out, corresponding to the three different chemical environments of coordination sites in the supramolecule, i.e., one on the outer rim edge, and two on the spoke. Characteristic up field shifts of all a, b, c6,6'' are exhibited on the spectrum by comparing with the metal free tpy contained ligands (Figure S1, 3, 4).[14k, 28] In the spectrum of **SW-1** (Figure 4a), the characteristic peak of amino protons of **SW-3** shown around 5.4 ppm disappeared; meanwhile, the new peak assigned to H^{I} of pyridinium ring and the obvious down-field shift of H^{I} together prove the full conversion of amino group to pyridinium group, during the formation of **SW-1**. Four sets of tpy protonic peaks are exhibited in the spectrum, corresponding to the additional layer of hexagonal ring by comparing with **SW-3**. Again, the characteristic high field a-d6,6'' protonic signals are displayed, indicating the full coordination of tpy groups with Zn(II) ions. In addition, all peaks of **SW-1** inner layer protons ($H^{\text{A-H}}$, a,b,c-tpy-*H*) locate in much high magnetic field area compared with the corresponding signals of **SW-3**, which could be attributed to the electron shielding effect from the hexagonal outer rim on these inner ring protons. A 2D diffusion-ordered NMR spectroscopy (2D-DOSY) analysis in d_6-DMSO reveals a single band at logD ≈ −10.5 (Figure S30), corresponding to a discrete architecture. For comparison, the measured logD value of **SW-3** is *ca.* -10.3 (Figure S32), corresponding to its much smaller diameter compared with **SW-1**. Using the modified Stocks–Einstein equation based on the oblate spheroid model (see Supporting Information for details),[29] the experimental radii, i.e., the semimajor radius of **SW-1** and **SW-3** were calculated as 4.1 nm and 2.6 nm, which are comparable with the results obtained from theoretical models (3.9 nm shown in Figure 6c, and 2.8 nm shown in Figure S54). The other NMR spectroscopic results are summarized in the SI, including 2D COSY, 2D NOESY, ^{13}C NMR spectra (Figs. S12-29).

Transmission electron microscopy (TEM) was further utilized to visualize individual supramolecules. Under TEM imaging, a series of dots with narrowly dispersed diameters was observed (Figure S50a). Zoomed-in image of one dot shows a hexagon flake shape with the measured diameter as *ca.* 7.0 nm, which is consistent with the molecular modeling result (Figure 6c). To obtain a higher resolution image of **SW-1**, ultrahigh-vacuum, low-temperature scanning tunneling microscopy (UHV-LT-STM) was utilized to study the supramolecules on Ag(111) surface. As shown in Figure 6a-b and Figure S51, high density of individual **SW-1** molecules are observed on the surface with hexagram shape, and the diameter of each hexagram is also around 7.0 nm (Figure 6a). Note that, the bright dots in each hexagram represent <tpy-Zn(II)-tpy> units due to their octahedral coordination structure and higher electron density around the metal ions. Two layers of bright lobes, i.e., a hexagonal outer rim and a hexagonal inner ring, can be clearly observed in Figure 6b. The larger lobes on the outer rim are assigned to the two layers of <tpy-Zn(II)-tpy> units with their signals merged together, while the smaller ones in the inner ring are attributed to the <tpy-Zn(II)-tpy> junctions linked to the hexatopic core (ligand **D**).

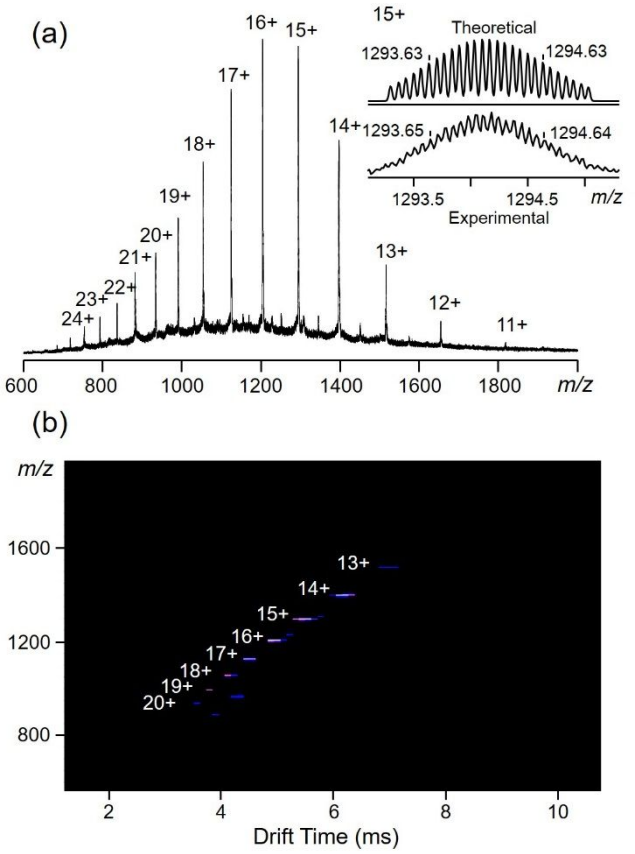

Figure 5. (a) Full ESI-MS spectrum with theoretical and experimental isotope patterns of 15+ species (right inset). (b) TWIM-MS (*m/z vs* drift time) of **SW-2**composed by four-component *in-situ* self-assembly strategy.

In addition to the hexatopic tpy ligand **D**, two tritopic tpy ligand **E** can act together as the cores to form another discrete supramolecular spiderweb (**SW-2**) with four-component synthesis/self-assembly in one pot, i.e., **A**/**C**/**D**/Zn, as shown in Scheme 2b.[30] ESI-MS spectrum of the resulted product (**Figure 5**) proves the structure with desired chemical composition ($C_{1002}H_{684}N_{114}Zn_{18}P_{42}F_{252}$), by displaying a series of sharp peaks with average measured molecular mass as 21,585 Da. And the experimental

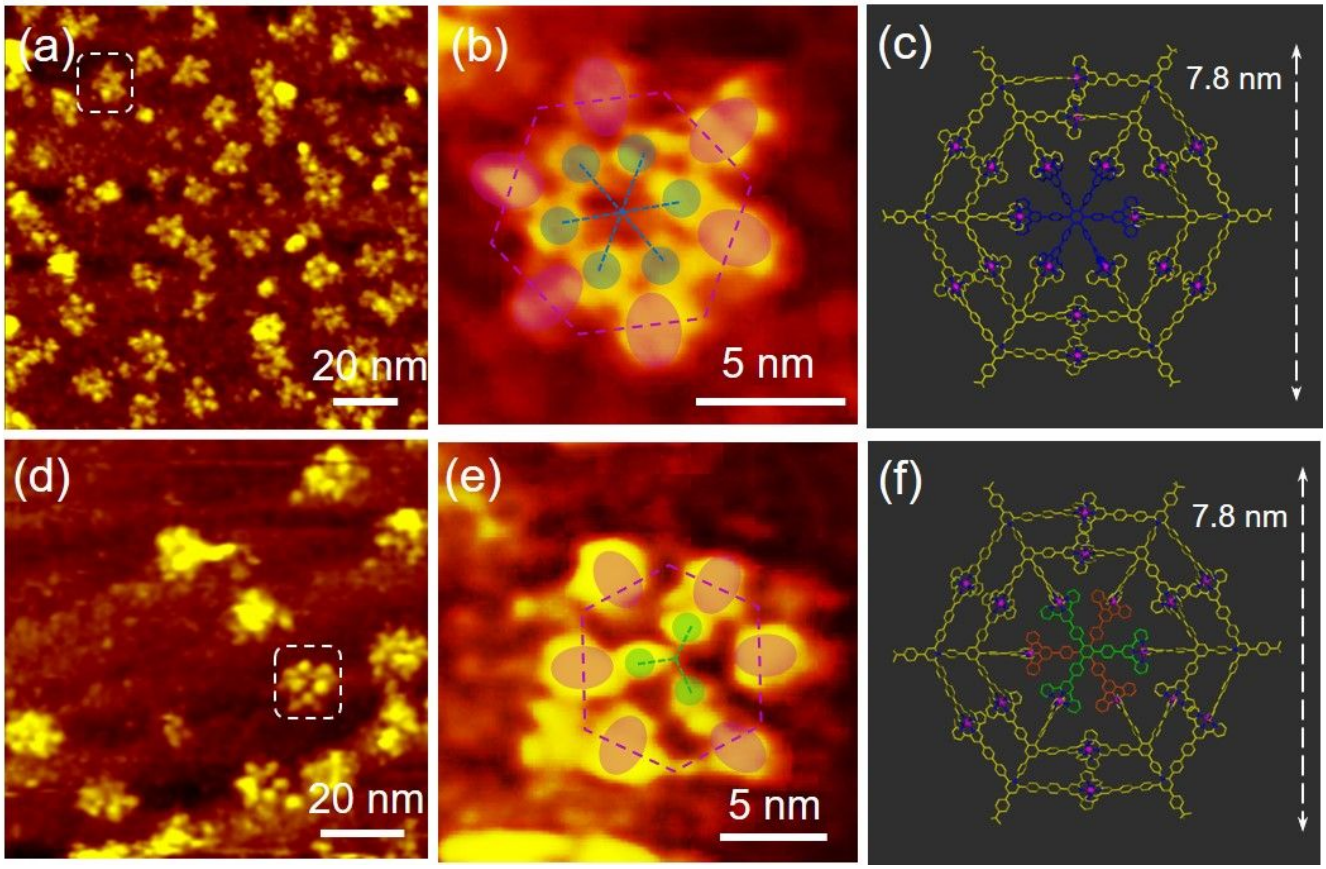

Figure 6. (a) STM image of individual **SW-1** on Ag(111) surface; (b) Zoomed-in STM image of one **SW-1** supramolecule in (a), (d) STM image of individual **SW-2** on Ag(111) surface; (e) Zoomed-in STM image of one **SW-2** supramolecule in (d); (c) and (f) representative energy-minimized structures from molecular modeling of **SW-1** and **SW-2**; alkyl chains were omitted for clarity. Dash lines covered on the images of (b) and (e) represent the organic backbone of the complexes, pink ovals represent the double-layers of <tpy-Zn(II)-tpy> junctions on the outer rim, and blue/green rounds correspond the <tpy-Zn(II)-tpy> junction linked to the core.

isotope patterns of each charge states are consistent with their corresponding theoretical ones (Figure 5 inset, and Figure S35). TWIM-MS spectra of **SW-2** also exhibits a narrowly distributed set of signal bands, corresponding to an averaged experimental CCS value as 2765.0 Å^2, in good agreement with the average theoretical CCS value as, 2761.8 Å^2 (as shown in Table S2, Figure S49). The total dissociation voltage of **SW-2** was measured with the same value as **SW-1** in gMS^2 spectra (40 V, Figure S40), owing to their similar DOCS values. The ^{1}H NMR spectrum of **SW-2** shows similar signals as that of **SW-1** (Figures S18-23) with four sets of tpy protonic resonance signals assigning to the four different chemical environments of tpy-Zn(II) coordination sites. 2D-DOSY spectrum of **SW-2** reveals a single band of signals with the same logD value of **SW-1** at *ca.* −10.5 (Figure S31) with calculated radius as 4.1 nm (Figure 6f). TEM and STM images of **SW-2** (Figure 6d-e, Figure S50b, S52) also clearly shows hexagonal shaped flakes of individual supramolecule with narrowly dispersed diameter at *ca.* 7.0 nm, further documenting the formation of desired structure. Zoomed-in STM image of **SW-2** (Figure 6d) also shows the pattern with six larger signal lobes arranged in the outer rim of a hexagon, and a triangular pattern in the inner ring. The observed inner patterns are attributed to the three coordination junctions attached to the upper level of tritopic core (ligand **E**), while the lower level of core cannot be detected by the tip.

With such a new strategy in hand, we further explored the selectivity of a more complicated system, i.e., selective assembly of **SW-1** in the system containing precursors **A/C/D/E** and metal ions Zn(II) with the molar ratio 6/6/1/2/18, as illustrated in Scheme 3a. Instead of forming a pool of mixtures, the five-component self-assembly precisely picked up **A/C/D/**Zn(II) with stoichiometric ratio to form pure **SW-1**. ESI-MS spectrum of the obtained assembled product displays only one dominant set of sharp peaks, which exactly matches the chemical composition of **SW-1** (Figure S46). Furthermore, complete core exchange was conducted by mixing equal amount of **SW-2** and hexatopic ligand **D** at 110 °C (Scheme 3b). But such an exchange procedure could not occur reversely by adding 2 eq. **E** into **SW-1** solution. Increasing the amount of **E** could only partially convert **SW-1** to **SW-2** with unidentified assemblies as revealed by the messy ESI-MS spectrum (Figure S47). All these results suggest that **SW-1** is a more energy favorable structure compared with **SW-2**. In this five-component system, a self-recognition was realized in the competition between **D** and **E**.

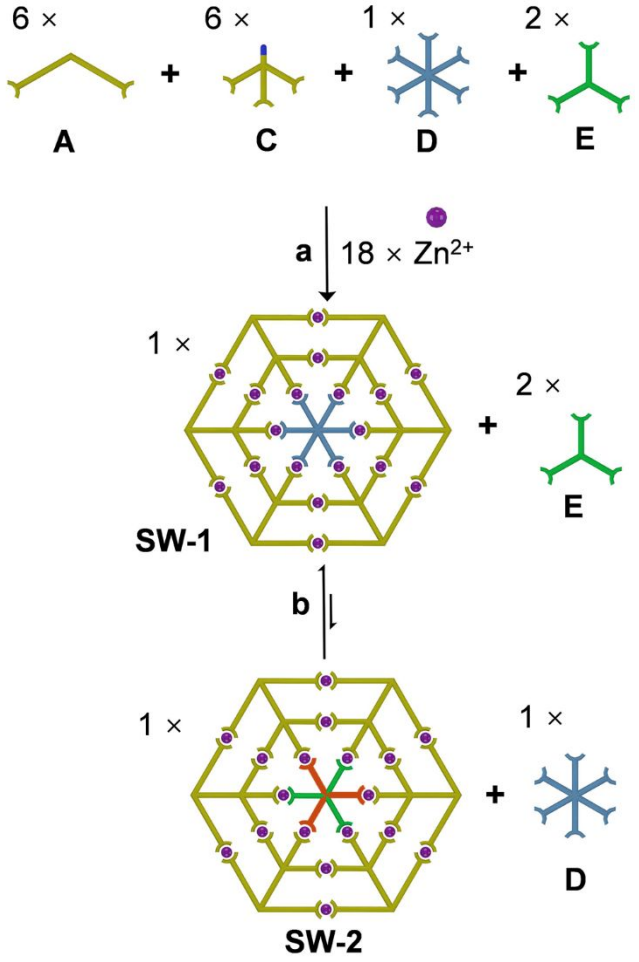

Scheme 3. (a) Selective assembly of **SW-1** through the synthesis/self-assembly in one pot strategy involving two core ligands **D** and **E**. (b) Transforming **SW-2** to **SW-1** by adding equal equivalency of **D**. Reaction condition: DMSO, 110 °C, 24 hours.

Conclusions

We demonstrate here a novel *in-situ* multi-component synthesis/self-assembly strategy by combining the irreversible pyrylium salt-primary amine condensation and the highly revisable tpy-Zn coordination, in an orthogonal way. A double layered supramolecular Kandinsky Circle and two supramolecular spiderwebs were constructed through the three-component and four-component synthesis/self-assembly in one-pot with high efficiency. It reveals that this one-pot strategy is a thermodynamically controlled process through monitoring the reaction procedure, as well as studying the core sorting/exchange behavior between **SW-1** and **SW-2** systems. Our endeavors expand the scope of the *in-situ* synthesis/self-assembly strategies from highly reversible reactions to irreversible ones. This new method can emerge as a powerful approach in building sophisticated supramolecular structures with high efficiency.

ASSOCIATED CONTENT

Supporting Information. Synthetic details, molecular modeling, ligand and complex characterization, including ^{1}H NMR, ^{13}C NMR, 2D COSY, 2D NOESY, 2D DOSY, ESI-MS, TWIM-MS and additional TEM and STM images are included in supporting information. This material is available free of charge via the Internet at http://pubs.acs.org.

AUTHOR INFORMATION

Corresponding Author

* xiaopengli1@usf.edu

Notes

The authors declare no competing financial interest

ACKNOWLEDGMENT

This research was supported by the National Science Foundation (CHE-1506722) and National Institutes of Health (R01GM128037). Use of the Center for Nanoscale Materials, an Office of Science user facility, was supported by the U.S. Department of Energy, Office of Science, Office of Basic Energy Sciences, under Contract No. DE-AC02-06CH11357. We also acknowledge partial support by University of South Florida Interdisciplinary NMR facility, and through a University of South Florida Nexus Initiative (UNI) Award.

REFERENCES

1. Alberts, B.; Johnson, A.; Lewis, J.; Raff, M.; Roberts, K.; Walter, P., *Molecular biology of the cell*. 6th Edition ed.; Garland Science: New York, 2014.
2. Whitesides, G. M.; Grzybowski, B., Self-Assembly at All Scales. *Science* **2002,** *295* (5564), 2418-2421.
3. (a) Leininger, S.; Olenyuk, B.; Stang, P. J., Self-Assembly of Discrete Cyclic Nanostructures Mediated by Transition Metals. *Chem. Rev.* **2000,** *100* (3), 853-908; (b) Chakrabarty, R.; Mukherjee, P. S.; Stang, P. J., Supramolecular Coordination: Self-Assembly of Finite Two- and Three-Dimensional Ensembles. *Chem. Rev.* **2011,** *111* (11), 6810-6918; (c) Cook, T. R.; Stang, P. J., Recent Developments in the Preparation and Chemistry of Metallacycles and Metallacages via Coordination. *Chem. Rev.* **2015,** *115* (15), 7001-7045.
4. (a) Hasenknopf, B.; Lehn, J.-M.; Kneisel, B. O.; Baum, G.; Fenske, D., Self-Assembly of a Circular Double Helicate. *Angew Chem. Int. Ed. Engl.* **1996,** *35* (16), 1838-1840; (b) Hasenknopf, B.; Lehn, J.-M.; Boumediene, N.; Dupont-Gervais, A.; Van Dorsselaer, A.; Kneisel, B.; Fenske, D., Self-Assembly of Tetra- and Hexanuclear Circular Helicates. *J. Am. Chem. Soc.* **1997,** *119* (45), 10956-10962; (c) Hasenknopf, B.; Lehn, J.-M.; Boumediene, N.; Leize, E.; Van Dorsselaer, A., Kinetic and Thermodynamic Control in Self-Assembly: Sequential Formation of Linear and Circular Helicates. *Angew. Chem. Int. Ed.* **1998,** *37* (23), 3265-3268; (d) Sørensen, A.; Castilla, A. M.; Ronson, T. K.; Pittelkow, M.; Nitschke, J. R., Chemical Signals Turn On Guest Binding through Structural Reconfiguration of Triangular Helicates. *Angew. Chem. Int. Ed.* **2013,** *52* (43), 11273-11277; (e) Ayme, J.-F.; Beves, J. E.; Campbell, C. J.; Leigh, D. A., The Self-Sorting Behavior of Circular Helicates and Molecular Knots and Links. *Angew. Chem. Int. Ed.* **2014,** *53* (30), 7823-7827.
5. (a) Bassani, D. M.; Lehn, J.-M.; Fromm, K.; Fenske, D., Toposelective and Chiroselective Self-Assembly of [2×2] Grid-Type Inorganic Arrays Containing Different Octahedral Metallic Centers. *Angew. Chem. Int. Ed.* **1998,** *37* (17), 2364-2367; (b) Toyota, S.; Woods, C. R.; Benaglia, M.; Haldimann, R.; Wärnmark, K.; Hardcastle, K.; Siegel, J. S., Tetranuclear Copper(I)-Biphenanthroline Gridwork: Violation of the Principle of Maximal Donor Coordination Caused by Intercalation and CH-to-N Forces.

Angew. Chem. Int. Ed. **2001,** *40* (4), 751-754; (c) Barboiu, M.; Vaughan, G.; Graff, R.; Lehn, J.-M., Self-Assembly, Structure, and Dynamic Interconversion of Metallosupramolecular Architectures Generated by Pb(II) Binding-Induced Unfolding of a Helical Ligand. *J. Am. Chem. Soc.* **2003,** *125* (34), 10257-10265.

6. (a) Kraus, T.; Buděšínský, M.; Cvačka, J.; Sauvage, J.-P., Copper(I)-Directed Formation of a Cyclic Pseudorotaxane Tetramer and Its Trimeric Homologue. *Angew. Chem. Int. Ed.* **2006,** *45* (2), 258-261; (b) Beyler, M.; Heitz, V.; Sauvage, J.-P., Coordination Chemistry-Assembled Porphyrinic Catenanes. *J. Am. Chem. Soc.* **2010,** *132* (12), 4409-4417; (c) Joosten, A.; Trolez, Y.; Collin, J.-P.; Heitz, V.; Sauvage, J.-P., Copper(I)-Assembled [3]Rotaxane Whose Two Rings Act as Flapping Wings. *J. Am. Chem. Soc.* **2012,** *134* (3), 1802-1809; (d) Yang, Y.-D.; Fan, C.-C.; Rambo, B. M.; Gong, H.-Y.; Xu, L.-J.; Xiang, J.-F.; Sessler, J. L., Multicomponent Self-Assembled Metal–Organic [3]Rotaxanes. *J. Am. Chem. Soc.* **2015,** *137* (40), 12966-12976; (e) Leigh, D. A.; Pirvu, L.; Schaufelberger, F.; Tetlow, D. J.; Zhang, L., Securing a Supramolecular Architecture by Tying a Stopper Knot. *Angew. Chem. Int. Ed.* **2018,** *57* (33), 10484-10488.

7. (a) Dietrich-Buchecker, C. O.; Sauvage, J. P.; Kintzinger, J. P., Une nouvelle famille de molecules : les metallo-catenanes. *Tetrahedron Lett.* **1983,** *24* (46), 5095-5098; (b) Dietrich-Buchecker, C. O.; Sauvage, J. P.; Kern, J. M., Templated synthesis of interlocked macrocyclic ligands: the catenands. *J. Am. Chem. Soc.* **1984,** *106* (10), 3043-3045.

8. Fujita, M.; Ibukuro, F.; Hagihara, H.; Ogura, K., Quantitative self-assembly of a [2]catenane from two preformed molecular rings. *Nature* **1994,** *367* (6465), 720-723.

9. (a) Freye, S.; Hey, J.; Torras-Galán, A.; Stalke, D.; Herbst-Irmer, R.; John, M.; Clever, G. H., Allosteric Binding of Halide Anions by a New Dimeric Interpenetrated Coordination Cage. *Angew. Chem. Int. Ed.* **2012,** *51* (9), 2191-2194; (b) Frank, M.; Hey, J.; Balcioglu, I.; Chen, Y.-S.; Stalke, D.; Suenobu, T.; Fukuzumi, S.; Frauendorf, H.; Clever, G. H., Assembly and Stepwise Oxidation of Interpenetrated Coordination Cages Based on Phenothiazine. *Angew. Chem. Int. Ed.* **2013,** *52* (38), 10102-10106; (c) Freye, S.; Michel, R.; Stalke, D.; Pawliczek, M.; Frauendorf, H.; Clever, G. H., Template Control over Dimerization and Guest Selectivity of Interpenetrated Coordination Cages. *J. Am. Chem. Soc.* **2013,** *135* (23), 8476-8479; (d) Zhu, R.; Lübben, J.; Dittrich, B.; Clever, G. H., Stepwise Halide-Triggered Double and Triple Catenation of Self-Assembled Coordination Cages. *Angew. Chem. Int. Ed.* **2015,** *54* (9), 2796-2800.

10. (a) Chichak, K. S.; Cantrill, S. J.; Pease, A. R.; Chiu, S.-H.; Cave, G. W. V.; Atwood, J. L.; Stoddart, J. F., Molecular Borromean Rings. *Science* **2004,** *304* (5675), 1308-1312; (b) Beves, J. E.; Campbell, C. J.; Leigh, D. A.; Pritchard, R. G., Tetrameric Cyclic Double Helicates as a Scaffold for a Molecular Solomon Link. *Angew. Chem. Int. Ed.* **2013,** *52* (25), 6464-6467; (c) Schouwey, C.; Holstein, J. J.; Scopelliti, R.; Zhurov, K. O.; Nagornov, K. O.; Tsybin, Y. O.; Smart, O. S.; Bricogne, G.; Severin, K., Self-Assembly of a Giant Molecular Solomon Link from 30 Subcomponents. *Angew. Chem. Int. Ed.* **2014,** *53* (42), 11261-11265.

11. (a) Guo, J.; Mayers, P. C.; Breault, G. A.; Hunter, C. A., Synthesis of a molecular trefoil knot by folding and closing on an octahedral coordination template. *Nat. Chem.* **2010,** *2*, 218; (b) Ayme, J.-F.; Beves, J. E.; Leigh, D. A.; McBurney, R. T.; Rissanen, K.; Schultz, D., A synthetic molecular pentafoil knot. *Nat. Chem.* **2011,** *4*, 15; (c) Barran, P. E.; Cole, H. L.; Goldup, S. M.; Leigh, D. A.; McGonigal, P. R.; Symes, M. D.; Wu, J.; Zengerle, M., Active-Metal Template Synthesis of a Molecular Trefoil Knot. *Angew. Chem. Int. Ed.* **2011,** *50* (51), 12280-12284; (d) Leigh, D. A.; Pritchard, R. G.; Stephens, A. J., A Star of David catenane. *Nat. Chem.* **2014,** *6*, 978; (e) Zhang, L.; Stephens, A. J.; Nussbaumer, A. L.; Lemonnier, J.-F.; Jurček, P.; Vitorica-Yrezabal, I. J.; Leigh, D. A., Stereoselective synthesis of a composite knot with nine crossings. *Nat. Chem.* **2018,** *10* (11), 1083-1088.

12. (a) Fujita, M.; Yazaki, J.; Ogura, K., Preparation of a macrocyclic polynuclear complex, $[(en)Pd(4,4'\text{-bpy})]_4(NO_3)_8$ (en = ethylenediamine, bpy = bipyridine), which recognizes an organic molecule in aqueous media. *J. Am. Chem. Soc.* **1990,** *112* (14), 5645-5647; (b) Fujita, M.; Nagao, S.; Iida, M.; Ogata, K.; Ogura, K., Palladium(II)-directed assembly of macrocyclic dinuclear complexes composed of $(en)Pd^{2+}$ and bis(4-pyridyl)-substituted bidentate ligands. Remarkable ability for molecular recognition of electron-rich aromatic guests. *J. Am. Chem. Soc.* **1993,** *115* (4), 1574-1576.

13. (a) Stang, P. J.; Cao, D. H., Transition Metal Based Cationic Molecular Boxes. Self-Assembly of Macrocyclic Platinum(II) and Palladium(II) Tetranuclear Complexes. *J. Am. Chem. Soc.* **1994,** *116* (11), 4981-4982; (b) Stang, P. J.; Cao, D. H.; Saito, S.; Arif, A. M., Self-Assembly of Cationic, Tetranuclear, Pt(II) and Pd(II) Macrocyclic Squares. x-ray Crystal Structure of $[Pt^{2+}(dppp)(4,4'\text{-bipyridyl})^{2-}OSO_2CF_3]_4$. *J. Am. Chem. Soc.* **1995,** *117* (23), 6273-6283; (c) Stang, P. J.; Chen, K., Hybrid, Iodonium-Transition Metal, Cationic Tetranuclear Macrocyclic Squares. *J. Am. Chem. Soc.* **1995,** *117* (5), 1667-1668; (d) Manna, J.; Whiteford, J. A.; Stang, P. J.; Muddiman, D. C.; Smith, R. D., Design and Self-Assembly of Nanoscale Organoplatinum Macrocycles. *J. Am. Chem. Soc.* **1996,** *118* (36), 8731-8732; (e) Stang, P. J.; Persky, N. E.; Manna, J., Molecular Architecture via Coordination: Self-Assembly of Nanoscale Platinum Containing Molecular Hexagons. *J. Am. Chem. Soc.* **1997,** *119* (20), 4777-4778; (f) Ghosh, K.; Yang, H.-B.; Northrop, B. H.; Lyndon, M. M.; Zheng, Y.-R.; Muddiman, D. C.; Stang, P. J., Coordination-Driven Self-Assembly of Cavity-Cored Multiple Crown Ether Derivatives and Poly[2]pseudorotaxanes. *J. Am. Chem. Soc.* **2008,** *130* (15), 5320-5334; (g) Chakrabarty, R.; Stang, P. J., Post-assembly Functionalization of Organoplatinum(II) Metallacycles via Copper-free Click Chemistry. *J. Am. Chem. Soc.* **2012,** *134* (36), 14738-14741.

14. (a) Chan, Y.-T.; Li, X.; Yu, J.; Carri, G. A.; Moorefield, C. N.; Newkome, G. R.; Wesdemiotis, C., Design, Synthesis, and Traveling Wave Ion Mobility Mass Spectrometry Characterization of Iron(II)– and Ruthenium(II)–Terpyridine Metallomacrocycles. *J. Am. Chem. Soc.* **2011,** *133* (31), 11967-11976; (b) Sautter, A.; Schmid, D. G.; Jung, G.; Würthner, F., A Triangle−Square Equilibrium of Metallosupramolecular Assemblies Based on Pd(II) and Pt(II) Corners and Diazadibenzoperylene Bridging Ligands. *J. Am. Chem. Soc.* **2001,** *123* (23), 5424-5430; (c) You, C.-C.; Würthner, F., Self-Assembly of Ferrocene-Functionalized Perylene Bisimide Bridging Ligands with Pt(II) Corner to Electrochemically Active Molecular Squares. *J. Am. Chem. Soc.* **2003,** *125* (32), 9716-9725; (d) Schulze, M.; Kunz, V.; Frischmann, P. D.; Würthner, F., A supramolecular ruthenium macrocycle with high catalytic activity for water oxidation that mechanistically mimics photosystem II. *Nat. Chem.* **2016,** *8*, 576; (e) Campos-Fernández, C. S.; Clérac, R.; Koomen, J. M.; Russell, D. H.; Dunbar, K. R., Fine-Tuning the Ring-Size of Metallacyclophanes: A Rational Approach to Molecular Pentagons. *J. Am. Chem. Soc.* **2001,** *123* (4), 773-774; (f) Campos-Fernández, C. S.; Schottel, B. L.; Chifotides, H. T.; Bera, J. K.; Bacsa, J.; Koomen, J. M.; Russell, D. H.; Dunbar, K. R., Anion Template Effect on the Self-Assembly and Interconversion of Metallacyclophanes. *J. Am. Chem. Soc.* **2005,** *127* (37), 12909-12923; (g) Chifotides, H. T.; Giles, I. D.; Dunbar, K. R., Supramolecular Architectures with π-Acidic 3,6-Bis(2-pyridyl)-1,2,4,5-tetrazine Cavities: Role of Anion−π Interactions in the Remarkable Stability of Fe(II) Metallacycles in Solution. *J. Am. Chem. Soc.* **2013,** *135* (8), 3039-3055; (h) Safarowsky, C.; Merz, L.; Rang, A.; Broekmann, P.; Hermann, B. A.; Schalley, C. A., Second-Order Templation: Ordered Deposition of Supramolecular Squares on a Chloride-Covered Cu(100) Surface. *Angew. Chem. Int. Ed.* **2004,** *43* (10), 1291-1294; (i) Jeong, K. S.; Kim, S. Y.; Shin, U.-S.; Kogej, M.; Hai, N. T. M.; Broekmann, P.; Jeong, N.; Kirchner, B.; Reiher, M.; Schalley, C. A., Synthesis of Chiral Self-Assembling Rhombs and Their Characterization in Solution, in the Gas Phase, and at the Liquid−Solid Interface. *J. Am. Chem. Soc.* **2005,** *127* (50), 17672-

17685; (j) Wang, M.; Wang, K.; Wang, C.; Huang, M.; Hao, X.-Q.; Shen, M.-Z.; Shi, G.-Q.; Zhang, Z.; Song, B.; Cisneros, A.; Song, M.-P.; Xu, B.; Li, X., Self-Assembly of Concentric Hexagons and Hierarchical Self-Assembly of Supramolecular Metal–Organic Nanoribbons at the Solid/Liquid Interface. *J. Am. Chem. Soc.* **2016,** *138* (29), 9258-9268; (k) Wang, H.; Qian, X.; Wang, K.; Su, M.; Haoyang, W.-W.; Jiang, X.; Brzozowski, R.; Wang, M.; Gao, X.; Li, Y.; Xu, B.; Eswara, P.; Hao, X.-Q.; Gong, W.; Hou, J.-L.; Cai, J.; Li, X., Supramolecular Kandinsky circles with high antibacterial activity. *Nat. Commun.* **2018,** *9* (1), 1815.

15. (a) Takeda, N.; Umemoto, K.; Yamaguchi, K.; Fujita, M., A nanometre-sized hexahedral coordination capsule assembled from 24 components. *Nature* **1999,** *398*, 794; (b) Tominaga, M.; Suzuki, K.; Kawano, M.; Kusukawa, T.; Ozeki, T.; Sakamoto, S.; Yamaguchi, K.; Fujita, M., Finite, Spherical Coordination Networks that Self-Organize from 36 Small Components. *Angew. Chem. Int. Ed.* **2004,** *43* (42), 5621-5625; (c) Sun, Q.-F.; Iwasa, J.; Ogawa, D.; Ishido, Y.; Sato, S.; Ozeki, T.; Sei, Y.; Yamaguchi, K.; Fujita, M., Self-Assembled $M_{24}L_{48}$ Polyhedra and Their Sharp Structural Switch upon Subtle Ligand Variation. *Science* **2010,** *328* (5982), 1144-1147; (d) Fujita, D.; Ueda, Y.; Sato, S.; Yokoyama, H.; Mizuno, N.; Kumasaka, T.; Fujita, M., Self-Assembly of M30L60 Icosidodecahedron. *Chem* **2016,** *1* (1), 91-101.

16. (a) Olenyuk, B.; Levin, M. D.; Whiteford, J. A.; Shield, J. E.; Stang, P. J., Self-Assembly of Nanoscopic Dodecahedra from 50 Predesigned Components. *J. Am. Chem. Soc.* **1999,** *121* (44), 10434-10435; (b) Olenyuk, B.; Whiteford, J. A.; Fechtenkötter, A.; Stang, P. J., Self-assembly of nanoscale cuboctahedra by coordination chemistry. *Nature* **1999,** *398*, 796; (c) Leininger, S.; Fan, J.; Schmitz, M.; Stang, P. J., Archimedean solids: Transition metal mediated rational self-assembly of supramolecular-truncated tetrahedra. *Proc. Natl. Acad. Sci. U.S.A.* **2000,** *97* (4), 1380-1384; (d) Kuehl, C. J.; Kryschenko, Y. K.; Radhakrishnan, U.; Seidel, S. R.; Huang, S. D.; Stang, P. J., Self-assembly of nanoscopic coordination cages of D_{3h} symmetry. *Proc. Natl. Acad. Sci. U.S.A.* **2002,** *99* (8), 4932-4936; (e) Yan, X.; Cook, T. R.; Wang, P.; Huang, F.; Stang, P. J., Highly emissive platinum(II) metallacages. *Nat. Chem.* **2015,** *7*, 342.

17. (a) Hiraoka, S.; Harano, K.; Shiro, M.; Ozawa, Y.; Yasuda, N.; Toriumi, K.; Shionoya, M., Isostructural Coordination Capsules for a Series of 10 Different d^5–d^{10} Transition-Metal Ions. *Angew. Chem.* **2006,** *118* (39), 6638-6641; (b) Clever, G. H.; Tashiro, S.; Shionoya, M., Light-Triggered Crystallization of a Molecular Host–Guest Complex. *J. Am. Chem. Soc.* **2010,** *132* (29), 9973-9975; (c) Han, M.; Luo, Y.; Damaschke, B.; Gómez, L.; Ribas, X.; Jose, A.; Peretzki, P.; Seibt, M.; Clever, G. H., Light-Controlled Interconversion between a Self-Assembled Triangle and a Rhombicuboctahedral Sphere. *Angew. Chem. Int. Ed.* **2016,** *55* (1), 445-449; (d) Bar, A. K.; Chakrabarty, R.; Mostafa, G.; Mukherjee, P. S., Self-Assembly of a Nanoscopic Pt12Fe12 Heterometallic Open Molecular Box Containing Six Porphyrin Walls. *Angew. Chem. Int. Ed.* **2008,** *47* (44), 8455-8459; (e) Mal, P.; Breiner, B.; Rissanen, K.; Nitschke, J. R., White Phosphorus Is Air-Stable Within a Self-Assembled Tetrahedral Capsule. *Science* **2009,** *324* (5935), 1697-1699; (f) Riddell, I. A.; Smulders, M. M. J.; Clegg, J. K.; Hristova, Y. R.; Breiner, B.; Thoburn, J. D.; Nitschke, J. R., Anion-induced reconstitution of a self-assembling system to express a chloride-binding Co10L15 pentagonal prism. *Nat. Chem.* **2012,** *4*, 751; (g) Rizzuto, F. J.; Nitschke, J. R., Stereochemical plasticity modulates cooperative binding in a CoII12L6 cuboctahedron. *Nat. Chem.* **2017,** *9*, 903; (h) Mosquera, J.; Szyszko, B.; Ho, S. K. Y.; Nitschke, J. R., Sequence-selective encapsulation and protection of long peptides by a self-assembled $Fe^{II}_8L_6$ cubic cage. *Nat. Commun.* **2017,** *8*, 14882; (i) Wang, M.; Wang, C.; Hao, X.-Q.; Li, X.; Vaughn, T. J.; Zhang, Y.-Y.; Yu, Y.; Li, Z.-Y.; Song, M.-P.; Yang, H.-B.; Li, X., From Trigonal Bipyramidal to Platonic Solids: Self-Assembly and Self-Sorting Study of Terpyridine-Based 3D Architectures. *J. Am. Chem. Soc.* **2014,** *136* (29), 10499-10507; (j) Xie, T.-Z.; Liao, S.-Y.; Guo, K.; Lu, X.; Dong, X.; Huang, M.; Moorefield, C. N.; Cheng, S. Z. D.; Liu, X.; Wesdemiotis, C.; Newkome, G. R., Construction of a Highly Symmetric Nanosphere via a One-Pot Reaction of a Tristerpyridine Ligand with Ru(II). *J. Am. Chem. Soc.* **2014,** *136* (23), 8165-8168; (k) Kaphan, D. M.; Levin, M. D.; Bergman, R. G.; Raymond, K. N.; Toste, F. D., A supramolecular microenvironment strategy for transition metal catalysis. *Science* **2015,** *350* (6265), 1235-1238; (l) Xie, T.-Z.; Guo, K.; Guo, Z.; Gao, W.-Y.; Wojtas, L.; Ning, G.-H.; Huang, M.; Lu, X.; Li, J.-Y.; Liao, S.-Y.; Chen, Y.-S.; Moorefield, C. N.; Saunders, M. J.; Cheng, S. Z. D.; Wesdemiotis, C.; Newkome, G. R., Precise Molecular Fission and Fusion: Quantitative Self-Assembly and Chemistry of a Metallo-Cuboctahedron. *Angew. Chem.* **2015,** *127* (32), 9356-9361; (m) Zhang, H.; Lee, J.; Lammer, A. D.; Chi, X.; Brewster, J. T.; Lynch, V. M.; Li, H.; Zhang, Z.; Sessler, J. L., Self-Assembled Pyridine-Dipyrrolate Cages. *J. Am. Chem. Soc.* **2016,** *138* (13), 4573-4579.

18. (a) Wang, M.; Zheng, Y.-R.; Ghosh, K.; Stang, P. J., Metallosupramolecular Tetragonal Prisms via Multicomponent Coordination-Driven Template-Free Self-Assembly. *J. Am. Chem. Soc.* **2010,** *132* (18), 6282-6283; (b) Zheng, Y.-R.; Zhao, Z.; Wang, M.; Ghosh, K.; Pollock, J. B.; Cook, T. R.; Stang, P. J., A Facile Approach toward Multicomponent Supramolecular Structures: Selective Self-Assembly via Charge Separation. *J. Am. Chem. Soc.* **2010,** *132* (47), 16873-16882.

19. (a) Mahata, K.; Schmittel, M., From 2-Fold Completive to Integrative Self-Sorting: A Five-Component Supramolecular Trapezoid. *J. Am. Chem. Soc.* **2009,** *131* (45), 16544-16554; (b) Saha, M. L.; Schmittel, M., From 3-Fold Completive Self-Sorting of a Nine-Component Library to a Seven-Component Scalene Quadrilateral. *J. Am. Chem. Soc.* **2013,** *135* (47), 17743-17746; (c) Mittal, N.; Pramanik, S.; Paul, I.; De, S.; Schmittel, M., Networking Nanoswitches for ON/OFF Control of Catalysis. *J. Am. Chem. Soc.* **2017,** *139* (12), 4270-4273.

20. Wang, S.-Y.; Fu, J.-H.; Liang, Y.-P.; He, Y.-J.; Chen, Y.-S.; Chan, Y.-T., Metallo-Supramolecular Self-Assembly of a Multicomponent Ditrigon Based on Complementary Terpyridine Ligand Pairing. *J. Am. Chem. Soc.* **2016,** *138* (11), 3651-3654.

21. (a) Nitschke, J. R., Construction, Substitution, and Sorting of Metallo-organic Structures via Subcomponent Self-Assembly. *Acc. Chem. Res.* **2007,** *40* (2), 103-112; (b) Sarma, R. J.; Nitschke, J. R., Self-Assembly in Systems of Subcomponents: Simple Rules, Subtle Consequences. *Angew. Chem. Int. Ed.* **2008,** *47* (2), 377-380; (c) Wood, C. S.; Ronson, T. K.; Belenguer, A. M.; Holstein, J. J.; Nitschke, J. R., Two-stage directed self-assembly of a cyclic [3]catenane. *Nat. Chem.* **2015,** *7*, 354; (d) Rizzuto, F. J.; Ramsay, W. J.; Nitschke, J. R., Otherwise Unstable Structures Self-Assemble in the Cavities of Cuboctahedral Coordination Cages. *J. Am. Chem. Soc.* **2018,** *140* (36), 11502-11509.

22. (a) Kumazawa, K.; Biradha, K.; Kusukawa, T.; Okano, T.; Fujita, M., Multicomponent Assembly of a Pyrazine-Pillared Coordination Cage That Selectively Binds Planar Guests by Intercalation. *Angew. Chem. Int. Ed.* **2003,** *42* (33), 3909-3913; (b) Kubota, Y.; Sakamoto, S.; Yamaguchi, K.; Fujita, M., Guest-induced organization of an optimal receptor from a dynamic receptor library: Spectroscopic screening. *Proc. Natl. Acad. Sci. U.S.A.* **2002,** *99* (8), 4854-4856.

23. (a) Bols, P. S.; Anderson, H. L., Template-Directed Synthesis of Molecular Nanorings and Cages. *Acc. Chem. Res.* **2018,** *51* (9), 2083-2092; (b) Hoffmann, M.; Wilson, C. J.; Odell, B.; Anderson, H. L., Template-Directed Synthesis of a π-Conjugated Porphyrin Nanoring. *Angew. Chem. Int. Ed.* **2007,** *46* (17), 3122-3125; (c) O'Sullivan, M. C.; Sprafke, J. K.; Kondratuk, D. V.; Rinfray, C.; Claridge, T. D. W.; Saywell, A.; Blunt, M. O.; O'Shea, J. N.; Beton, P. H.; Malfois, M.; Anderson, H. L., Vernier templating and synthesis of a 12-porphyrin nano-ring. *Nature* **2011,** *469*, 72; (d) Kondratuk, D. V.; Perdigão, L. M. A.; Esmail, A. M. S.; O'Shea, J. N.; Beton, P. H.; Anderson, H. L., Supramolecular nesting of cyclic polymers. *Nat. Chem.* **2015,** *7*, 317; (e) Neuhaus, P.; Cnossen, A.; Gong, J. Q.; Herz, L. M.; Anderson, H. L., A Molecular Nanotube with Three-Dimensional π-Conjugation. *Angew. Chem. Int. Ed.* **2015,** *54* (25), 7344-7348; (f) Cremers, J.; Haver, R.; Rickhaus, M.; Gong, J. Q.;

Favereau, L.; Peeks, M. D.; Claridge, T. D. W.; Herz, L. M.; Anderson, H. L., Template-Directed Synthesis of a Conjugated Zinc Porphyrin Nanoball. *J. Am. Chem. Soc.* **2018,** *140* (16), 5352-5355.

24. (a) Katritzky, A. R.; Manzo, R. H., Kinetics and mechanism of the reactions of primary amines with pyrylium cations. *J. Chem. Soc., Perkin Trans. 2* **1981,** (3), 571-575; (b) Katritzky, A. R.; Manzo, R. H.; Lloyd, J. M.; Patel, R. C., Mechanism of the Pyrylium/Pyridinium Ring Interconversion. Mild Preparative Conditions for Conversion of Amines into Pyridinium Ions. *Angew Chem. Int. Ed. Engl.* **1980,** *19* (4), 306-306.

25. (a) Chakraborty, S.; Newkome, G. R., Terpyridine-based metallosupramolecular constructs: tailored monomers to precise 2D-motifs and 3D-metallocages. *Chem. Soc. Review.* **2018,** *47* (11), 3991-4016; (b) Xie, T.-Z.; Endres, K. J.; Guo, Z.; Ludlow, J. M.; Moorefield, C. N.; Saunders, M. J.; Wesdemiotis, C.; Newkome, G. R., Controlled Interconversion of Superposed-Bistriangle, Octahedron, and Cuboctahedron Cages Constructed Using a Single, Terpyridinyl-Based Polyligand and Zn^{2+}. *J. Am. Chem. Soc.* **2016,** *138* (38), 12344-12347.

26. (a) Brocker, E. R.; Anderson, S. E.; Northrop, B. H.; Stang, P. J.; Bowers, M. T., Structures of Metallosupramolecular Coordination Assemblies Can Be Obtained by Ion Mobility Spectrometry–Mass Spectrometry. *J. Am. Chem. Soc.* **2010,** *132* (38), 13486-13494; (b) Li, X.; Chan, Y.-T.; Newkome, G. R.; Wesdemiotis, C., Gradient Tandem Mass Spectrometry Interfaced with Ion Mobility Separation for the Characterization of Supramolecular Architectures. *Anal. Chem.* **2011,** *83* (4), 1284-1290; (c) Thalassinos, K.; Grabenauer, M.; Slade, S. E.; Hilton, G. R.; Bowers, M. T.; Scrivens, J. H., Characterization of Phosphorylated Peptides Using Traveling Wave-Based and Drift Cell Ion Mobility Mass Spectrometry. *Anal. Chem.* **2009,** *81* (1), 248-254.

27. Sun, B.; Wang, M.; Lou, Z.; Huang, M.; Xu, C.; Li, X.; Chen, L.-J.; Yu, Y.; Davis, G. L.; Xu, B.; Yang, H.-B.; Li, X., From Ring-in-Ring to Sphere-in-Sphere: Self-Assembly of Discrete 2D and 3D Architectures with Increasing Stability. *J. Am. Chem. Soc.* **2015,** *137* (4), 1556-1564.

28. Wang, J.-L.; Li, X.; Lu, X.; Hsieh, I. F.; Cao, Y.; Moorefield, C. N.; Wesdemiotis, C.; Cheng, S. Z. D.; Newkome, G. R., Stoichiometric Self-Assembly of Shape-Persistent 2D Complexes: A Facile Route to a Symmetric Supramacromolecular Spoked Wheel. *J. Am. Chem. Soc.* **2011,** *133* (30), 11450-11453.

29. (a) Giuseppone, N.; Schmitt, J.-L.; Allouche, L.; Lehn, J.-M., DOSY NMR Experiments as a Tool for the Analysis of Constitutional and Motional Dynamic Processes: Implementation for the Driven Evolution of Dynamic Combinatorial Libraries of Helical Strands. *Angew. Chem. Int. Ed.* **2008,** *47* (12), 2235-2239; (b) Schulze, B. M.; Watkins, D. L.; Zhang, J.; Ghiviriga, I.; Castellano, R. K., Estimating the shape and size of supramolecular assemblies by variable temperature diffusion ordered spectroscopy. *Org. Biomol. Chem.* **2014,** *12* (40), 7932-7936.

30. Lu, X.; Li, X.; Cao, Y.; Schultz, A.; Wang, J.-L.; Moorefield, C. N.; Wesdemiotis, C.; Cheng, S. Z. D.; Newkome, G. R., Self-Assembly of a Supramolecular, Three-Dimensional, Spoked, Bicycle-like Wheel. *Angew. Chem. Int. Ed.* **2013,** *52* (30), 7728-7731.

Table of Contents artwork

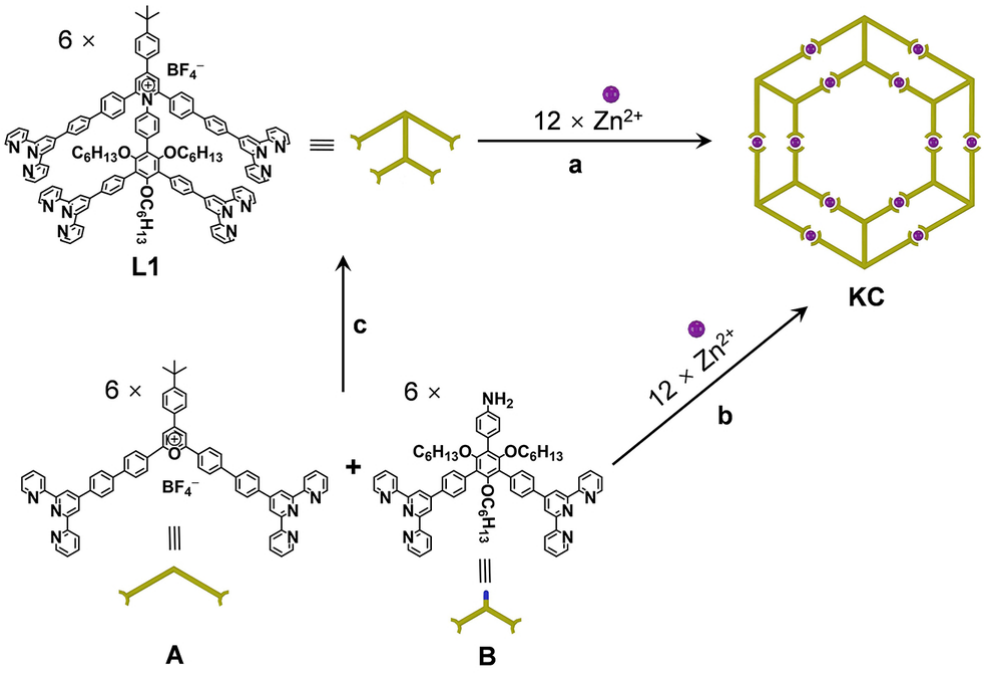

Scheme 1.Preparation of KC. (a) Conventional self-assembly using presynthesized ligand **L1**; condition: $CHCl_3$/MeOH (1/3, v/v), 50 ℃, 3 hours. (b) One-pot ap-proach with synthesis and self-assembly together using precursors **A** and **B**; condition: DMSO, 110 ℃, 24 hours. (c) Synthesis of **L1** from **A** and **B**, condition: DMSO, 120 ℃, 24 hours.

84x56mm (300 x 300 DPI)

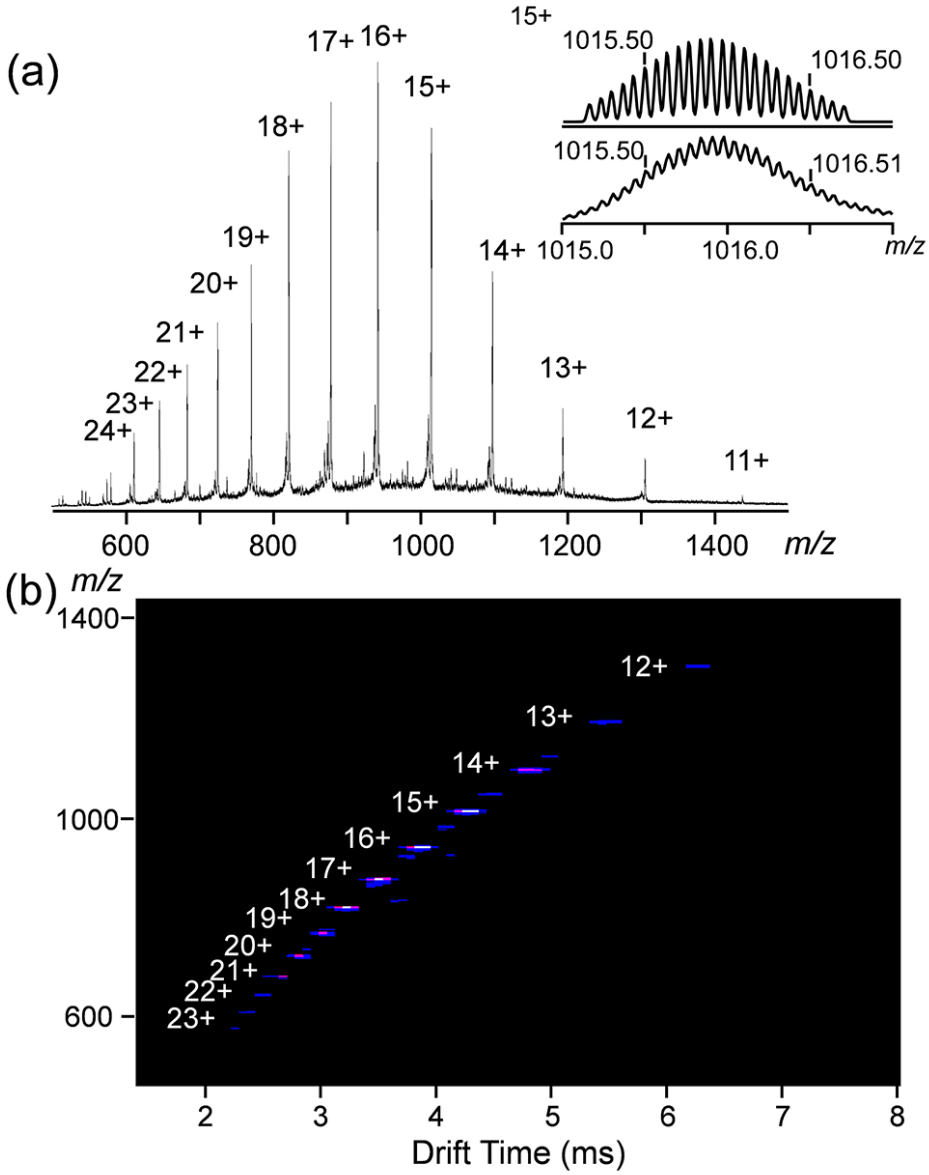

Figure 1. (a) Full ESI-MS spectrum with theoretical and experimental isotope patterns of 15+ species (right inset). (b) TWIM-MS (*m/z* vs drift time) of **KC** composed by three-component in-situ self-assembly strategy.

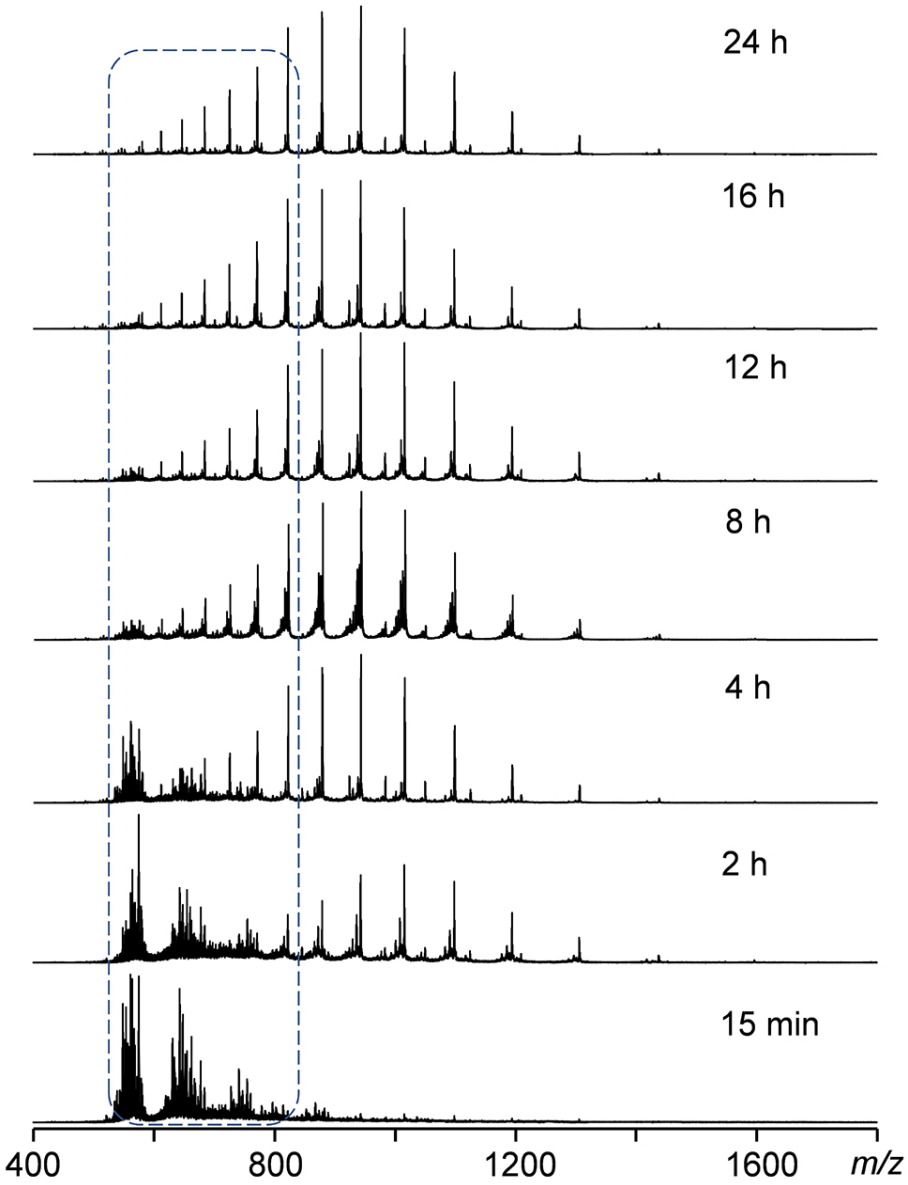

Figure 2. One-pot synthesis of **KC** at 110 ℃ monitored via ESI-MS at various reaction time.

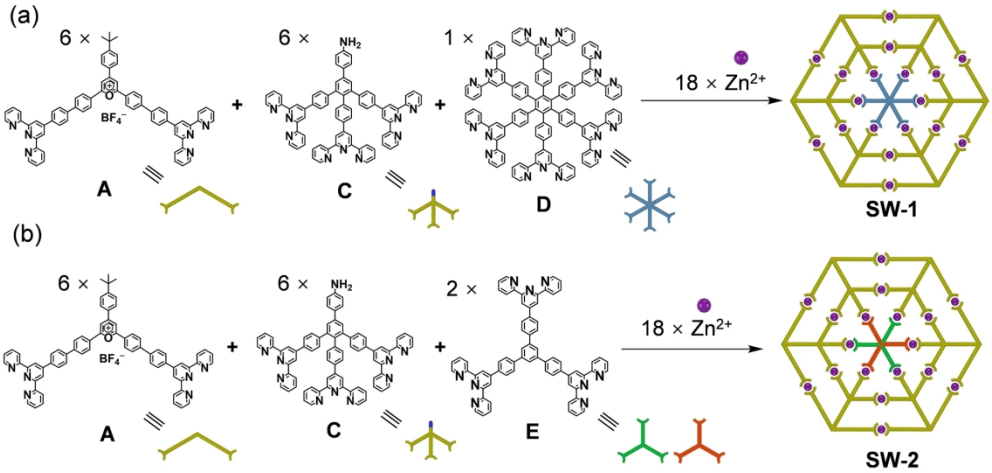

Scheme 2. Preparation of (a) SW-1 and (b) SW-2 through four-component synthesis/self-assembly in one pot. Condition: DMSO, 110 ℃, 24 hours.

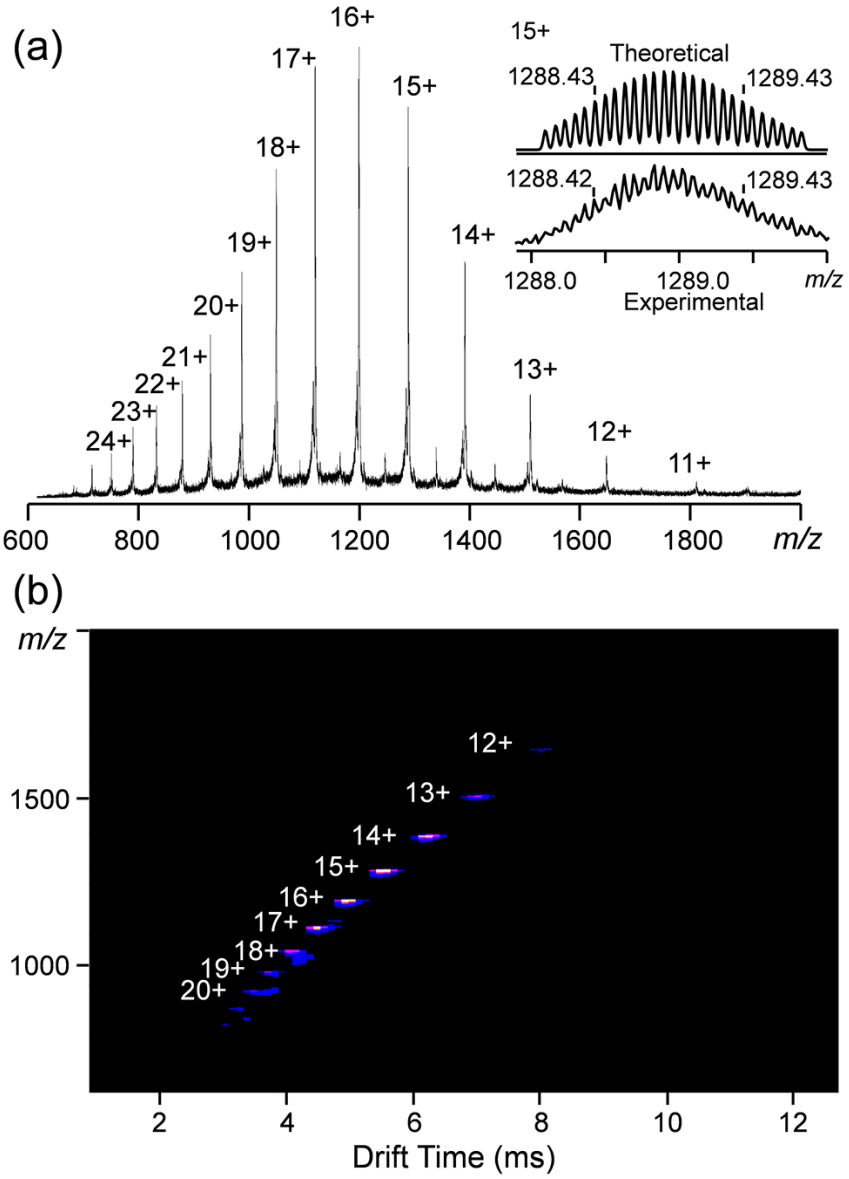

Figure 3. (a) Full ESI-MS spectrum with theoretical and experimental isotope patterns of 15+ species (right inset). (b) TWIM-MS (*m/z* vs drift time) of **SW-1** composed by four-component in-situ self-assembly strategy.

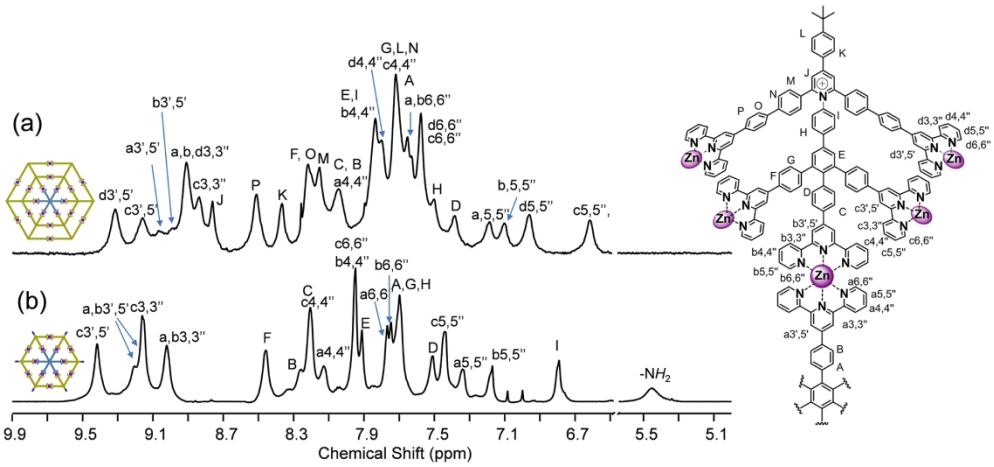

Figure 4. ^{1}H NMR spectra (600 MHz, d_6-DMSO, 300 K) of (a) **SW-1** and (b) **SW-3**.

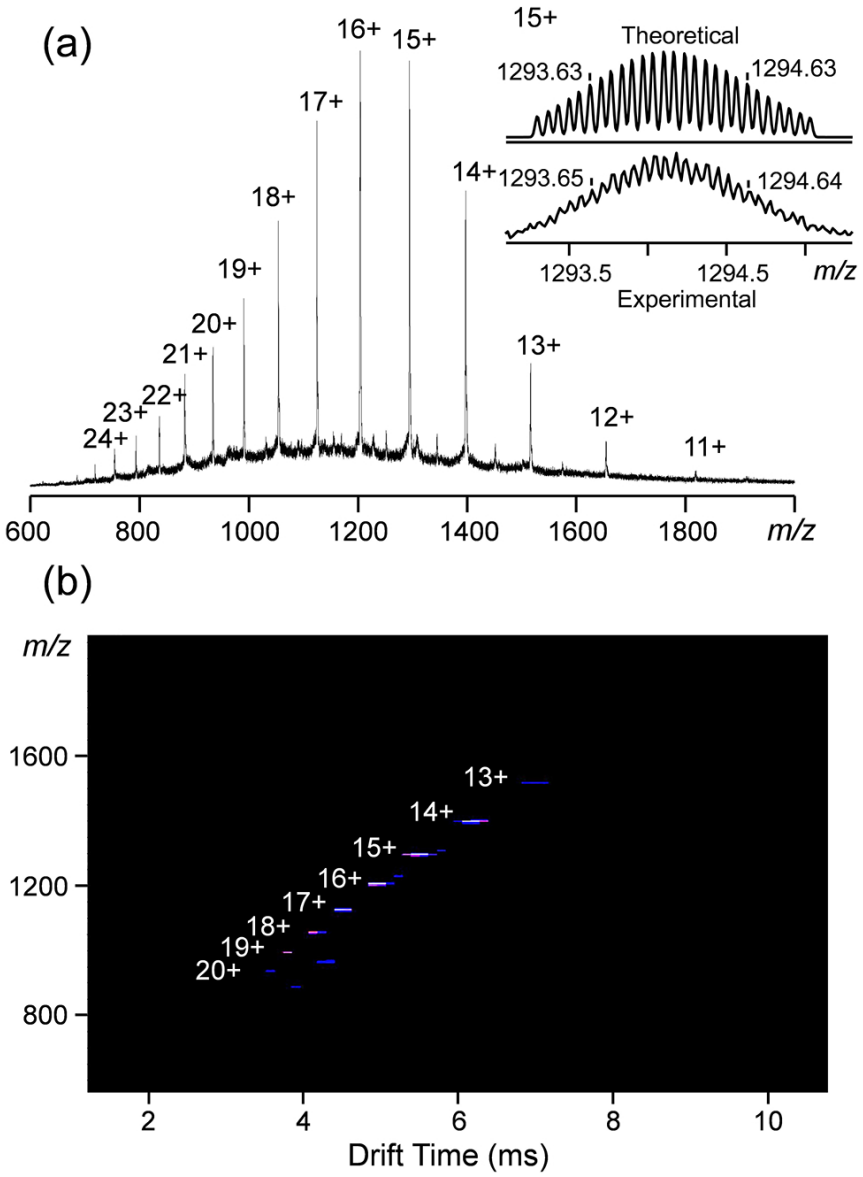

Figure 5. (a) Full ESI-MS spectrum with theoretical and experimental isotope patterns of 15+ species (right inset). (b) TWIM-MS (*m/z* vs drift time) of **SW-2** composed by four-component in-situ self-assembly strategy.

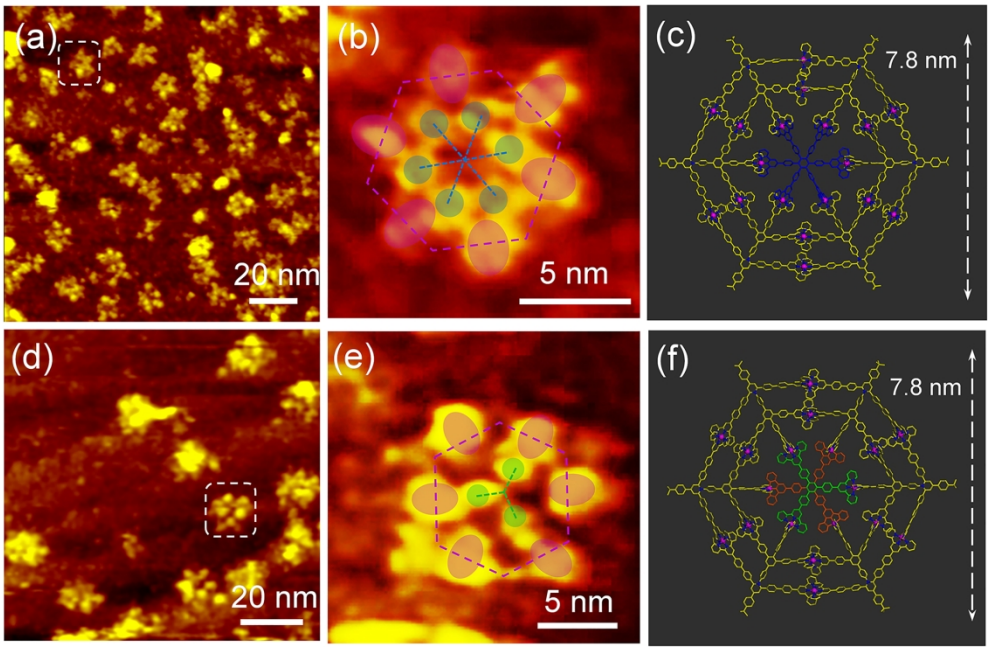

Figure 6. (a) STM image of individual **SW-1** on Ag(111) surface; (b) Zoomed-in STM image of one **SW-1** supramolecule in (a), (d) STM image of individual **SW-2** on Ag(111) surface; (e) Zoomed-in STM image of one **SW-2** supramolecule in (d); (c) and (f) representative energy-minimized structures from molecular modeling of **SW-1** and **SW-2**; alkyl chains were omitted for clarity. Dash lines covered on the images of (b) and (e) represent the organic backbone of the complexes, pink ovals represent the double-layers of <tpy-Zn(II)-tpy> junctions on the outer rim, and blue/green rounds correspond the <tpy-Zn(II)-tpy> junction linked to the core.

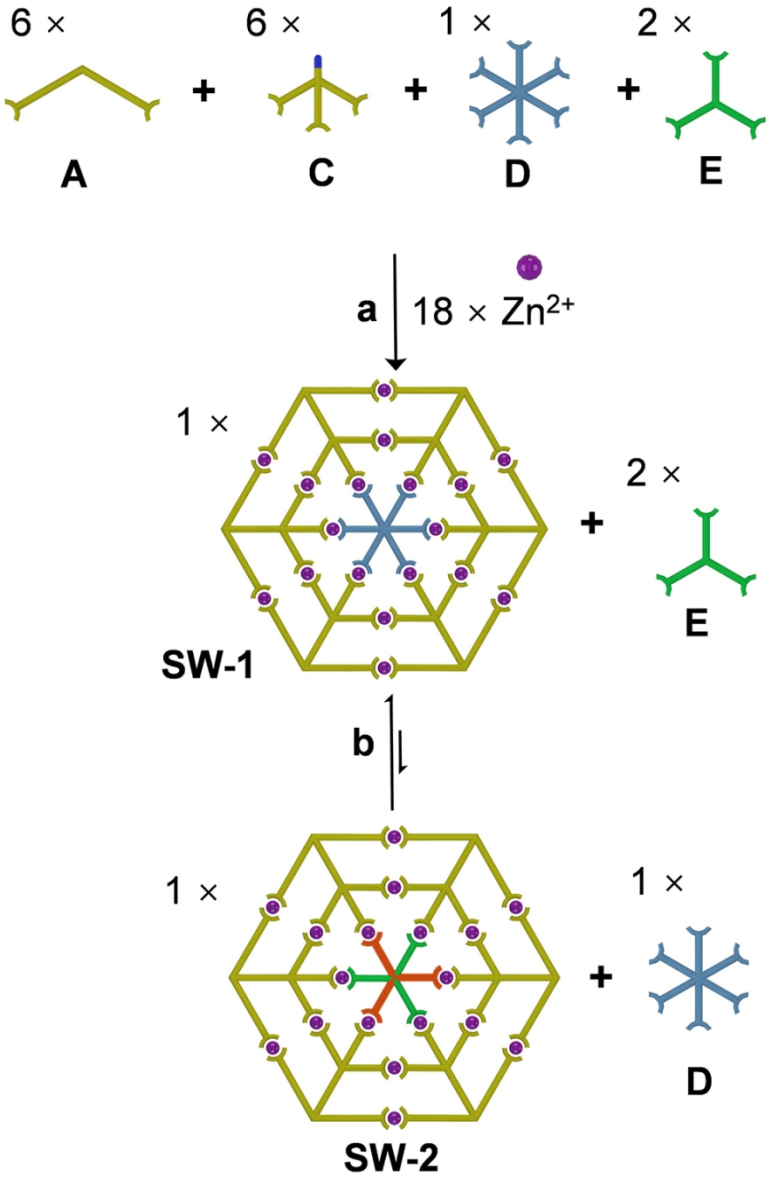

Scheme 3. (a) Selective assembly of **SW-1** through the synthesis/self-assembly in one pot strategy involving two core ligands **D** and **E**. (b) Transforming **SW-2** to **SW-1** by adding equal equivalency of **D**. Reaction condition: DMSO, 110 ℃, 24 hours.